the ant was quick to lose interest in its quarry. It paused momentarily to palpate the shield and sometimes even to bite into it (Fig. 1D), but eventually the ant always abandoned the attack and walked away.

In only two of the several dozen encounters witnessed did an ant succeed in biting a larva before the shield was mobilized against it. In one of these cases the larva was fatally injured, but in the other the ant held on only momentarily. Prodded by the shield, it relinquished its hold, briefly shifted its attention to the shield itself, and departed.

The presence of fresh wet feces near their site of deposition at the base of the shield (Fig. 1B) adds to the defense potential of the weapon. Ants that made casual contact with this pasty material when they first encountered the larva, or those that had it smeared upon them by the activated shield, usually fled promptly. During their escape they often paused to clean appendages or to drag their contaminated mouthparts against the substrate. Ants are known to react in this fashion to chemical repellents (*4*).

Larvae that had been artificially deprived of their shield were highly vulnerable. They attempted to defend themselves by maneuvering the naked fork, but they were nevertheless bitten and killed, or carried away live into the ant's nest (Fig. 1E).

Judging from its effect on ants, one might expect the shield to be deterrent also to other small predators. Yet it does not protect against all of them. Tests with an unidentified lycosid spider invariably resulted in the larva's being crushed by the chelicerae and sucked dry. Vulnerability to spiders had already been reported for the larva of another species of *Cassida* (*2*). It has been suggested, with some evidence (*5*), that the shield also protects against entomophagous parasites. But effectiveness is here again not absolute. Our own populations of *Cassida* were heavily parasitized by a chalcidoid wasp (*Tetrastichus* sp.).

THOMAS EISNER
EILEEN VAN TASSELL
JAMES E. CARREL
*Division of Biological Sciences, Cornell University, Ithaca, New York*

**References and Notes**

1. J. Weise, *Naturgeschichte Insekten Deut.* **6**, 1065 (1893).
2. H. Engel, *Z. Morphol. Okol. Tiere* **30**, 41 (1935).
3. B. D. Walsh and C. V. Riley, *Amer. Entomol.* **1**, 234 (1869).
4. T. Eisner and J. Meinwald, *Science* **153**, 1341 (1966).
5. J. Franz, *Anz. Schädlingskunde* **17**, 4 (1941), and references therein.
6. Study supported by NIH grant AI-02908.

1 September 1967

## Fast Potential Spike of Frog Skin Generated at the Outer Surface of the Epithelium

Abstract. *Experiments were performed to test which structure of frog skin epithelium is responsible for the electrical excitation (fast, all-or-none potential spike) displayed by this tissue during stimulation with a current pulse. Preselected cells of the outer epithelial surface were punctured by microelectrodes under microscopical observation. The major part of the transepithelia resting resistance and the major part of the spike were recorded between microelectrode tip and outside bathing solution. A leak between microelectrode and punctured membrane is made responsible for the attenuation of spike amplitude observed under these recording conditions. It is shown that if the spike is generated at but one of the series membranes of the epithelium, this membrane must be at the outermost border of the tissue.*

During the passage of constant inward current the transepithelial electrical potential of frog skin develops a spike-shaped all-or-none transient with a duration of about 10 msec and an amplitude of 200 mv. Its rising phase is characterized by an impedance increase, while its falling phase shows an impedance drop followed by a refractory state of depressed d-c resistance lasting up to 1 minute (*1*). Presently, we prefer to use the merely descriptive term "potential spike" for this phenomenon (*2*). Requisites for the spike are: (i) the presence of $Li^+$ or $Na^+$ in the solution bathing the outside of the skin, and (ii) an inward current density sufficiently high to bring the potential to a threshold value (*1*). The spike is of interest because of its similarity to the hyperpolarizing response of nerve and muscle plasma membranes. Also, its study may further illuminate the permeability properties of frog skin epithelium. In order to determine where in the epithelium (*3*) the transient impedance changes take place we used microelectrodes, the tips of which were inserted into individual, preselected surface cells under microscopical observation. The experimental arrangement is shown in Fig. 1. With transillumination and a magnification of 400, nuclei and cellular borders of the outermost cell layer were clearly discernible. When necessary, the contrast of these structures was improved by phase contrast or by vital staining with basic dyes. For staining, a few crystals of methylene blue or toluidine blue were added to the outside solution and washed away after a few minutes. Dye accumulated at the "chicken fence," in cellular nuclei, mainly in the second cellular layer below the outer surface, and in the lumen and cellular nuclei of the ducts of subepithelial glands. The degree of staining varied among skins, possibly depending on the regenerative phase of each epithelium. Acid dyes were ineffective, except fluorescein, which would sometimes stain the chicken fence and nuclei of the surface cellular layer when added to the outside solution. No harmful effects were noted when concentration of dye and time of exposure were kept low (*4*).

The surface cells had diameters of 20 to 40 $\mu$ when viewed from above (Fig. 1) and were 5 to 10 $\mu$ deep. Their depth was measured in unfixed 10-$\mu$ sections of rapidly frozen epithelia after reimmersion in Ringer fluid, by use of phase-contrast or dark-field microscopy. The total thickness of the epithelia was 40 to 60 $\mu$ in these sections or when estimated by means of the microscope focus (*5*) in the living preparation.

The solution facing the corium (inside solution) was isotonic chloride-Ringer, while that facing the outer epithelial surface was either isotonic chloride-Ringer or this solution diluted tenfold with distilled water. The probing electrode tip resistance of 5 to 50 megohms was monitored with a repetitive calibration pulse (pulse *A* of Figs. 2 and 3) of 1 msec duration, applied to the input of the microelectrode follower stage (*6*). This pulse was followed in time by a 25-msec rectangular current pulse of subrheobase strength (pulse *B*) passed inward through the epithelium between Ag-AgCl electrodes on either side of the skin. The overall skin potential (*V*)

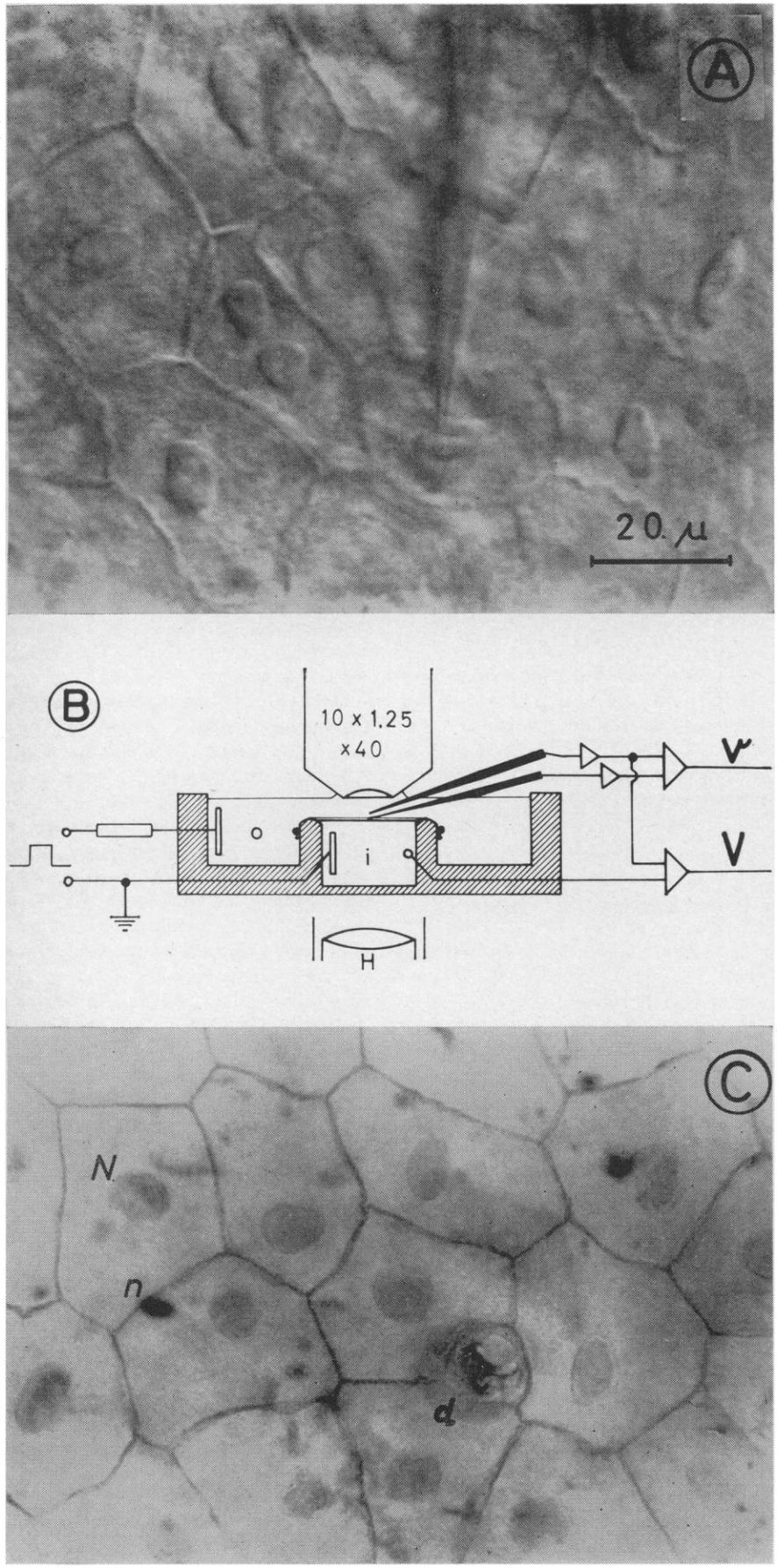


and the potentials between microelectrode and outer or inner reference electrode ($v$, or $V$-$v$) were concurrently displayed with a dual-beam oscilloscope. The pulse repetition rate was 2 per second. Characteristic traces were stored on the screen of a second oscilloscope and were subsequently photographed.

In Fig. 2, microelectrode resistance (pulse *A*) and the potential response ($V$-$v$) of the tissue layer between microelectrode tip and inside solution to overall stimulation of the epithelium with the repetitive current pulse *B* are shown for three different positions of the probing microelectrode tip. The tip was advanced (at first through the outer solution) at an angle of 30° to the epithelial surface (*7*) by means of a micromanipulator having a calibrated axial drive (*8*). Trace 1 is the transepithelial potential, recorded before the outer surface of the tissue was touched by the microelectrode tip. When the tip was advanced further, pulse *A* would suddenly indicate an increase of the tip resistance. At the same time a slight dimpling of one surface cell was usually seen, indicating that the tip was in contact with the outer border of the epithelium. The electrode advance was stopped at that moment and a reading was taken from the micrometer of the axial drive. When the electrode was advanced further, the tip resistance increased while the surface of the cell selected for penetration was further dimpled. The degree of dimpling is

Fig. 1 (left). (A) Unfixed, unstained cells of the outer layer, photographed from above with phase-contrast in the experimental lucite chamber shown below. For photographic purposes, the abdominal skin was replaced by the isolated vocal sac, which is more transparent and shows similar excitation phenomena; focus on chicken fence of outer epithelium. The microelectrode shank is seen to dimple the surface membrane of one cell while the tip deforms the cellular nucleus. (B) Schematic section through the experimental setup. The skin is tied onto the lucite chamber with the outer epithelial surface facing upward. Its distance from the microscope stage is 5 mm. Below the objective, the tip of the probing microelectrode is inserted into a surface cell. The other microelectrode monitors the reference potential above the cell impaled. Abbreviations: *o* and *i*, outer and inner bathing solution; *H*, Heine condensor. (C) Surface of abdominal skin slightly stained with methylene blue. *N*, nucleus in uppermost cellular layer; *n*, nucleus in layer below; and *d*, duct of subepithelial gland.

seen in Fig. 1, and usually involved no more than the surface of one cell. It caused large distortions of the microelectrode recording trace (trace 2). In most cases the deformation of the cell surface and the distortion of the recording trace were transient, and the previous tip resistance returned when the electrode tip was advanced further to a total distance of about 10 $\mu$, and then pulled back 2 to 5 $\mu$ (*9*). The surface dimpling was thus reduced, and the level of the record changed from the unsteady and displaced level associated with a deformed or obstructed microelectrode tip to a steady value, which was negative, positive, or unchanged with respect to the potential of the outer solution. It is difficult to determine how much a change of tip potential, caused by the composition of the cell interior, may have contributed to this d-c value.

With the tip in this position the *V-v* microelectrode recording showed that only 10 to 50 percent of the apparent epithelial d-c resistance remained between the microelectrode tip and the inner solution (trace 3). This percentage, the ease of tip-penetration, and the extent of vital staining varied among skins and may depend on the stage of an epithelium in its monthly regeneration cycle (*10*). Recordings similar to trace 3 were sometimes obtained even when the microelectrode was pulled back most of the 10 $\mu$ by which it had previously been advanced. When the electrode was backed off further, the recording usually would suddenly reassume the aspect of trace 1. In other experiments the electrode would apparently fail to completely obstruct the hole of entry through the membrane after the microelectrode had been withdrawn slightly. Records typical for extraepithelial tip positions (trace 1) were then obtained, although the tip was still clearly inside the surface cell. When the probing electrode was further advanced rather than withdrawn, its tip resistance increased again as the next cellular membrane was dimpled and penetrated (trace 2). It has been reported that the major resistive barrier of the epithelium is found at the outer surface of the sodium-transporting cellular layer, separated from the outer solution by layers of cornified, "dying" cells (*11*). However, in most epithelia investigated by us, the main resistive barrier appeared to be at the outermost surface of the epithelium. Possibly, the layers of cornified, "dying" cells seen by others were missing in our preparations.

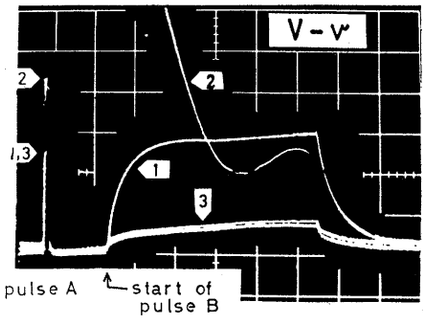


Fig. 2. Potential (*V-v*) between advancing microelectrode tip and solution bathing the inner side of the skin. Horizontal calibration: 5 msec per interval. Vertical calibration: pulse *A*, $10^7$ ohm per interval; pulse *B*, 50 mv per interval. Density of repetitive inward current pulse: 30 $\mu$a/cm$^2$.

It could be argued that the microelectrode tip, after passing through the outermost membrane had not yet penetrated a major resistive barrier but merely damaged such a barrier which, however, remained in front of the tip. The resulting drop of local epithelial resistance between tip and inner solution might qualitatively explain the response shown in Fig. 2. However, since more of the total current would flow through the area of low resistance, this mechanism can hardly explain the large potential difference between curves 1 and 3, even when Ringer diluted tenfold was used as the outer bathing solution. To get independent information on the resistance of the outermost membrane, three microelectrode tips were placed above one cell of the outermost layer (which was covered with isotonic chloride-Ringer). Electrode 1 delivered 5-msec pulses of constant current ($10^{-7}$ amp) to ground (the inner bathing solution was grounded); electrode 2 recorded the local potential of the outer solution with respect to ground; and electrode 3 was not connected to electronic devices. As long as tip 1 remained outside of the cell, a potential pulse could be recorded with electrode 2. However, when tip 1 was pushed through the outermost membrane, only less than 5 percent of the former signal amplitude was picked up by electrode 2. This loss of signal might be due to a local decrease of resistances between tip 1 and the inside solution if the signal is affected in the same way when tip 3, instead of tip 1, is pushed into the cell. However, with tip 1 and tip 2 outside the cell, the signal was not changed when tip 3 was pushed into the cell or withdrawn from it (*12*). We conclude that tip 1 passed a major resistive barrier when pushed through the outermost membrane.

In further experiments a different approach was used (Fig. 3A). The recording microelectrode was first lowered onto the tissue with its shank nearly parallel to the tissue surface until the tip section lay flat on the surface, slightly depressing the outer membranes of the surface cells. The tip was then advanced axially into the selected cell, entering it from the side rather than from above, and almost parallel to its upward-facing boundary. When manipulated in this way, the outer surface of the tissue gives the impression of a cobblestone surface (see Fig. 3A), which does not always seem to be preserved in sections of fixed cell layers. During entry the tip traveled from the edge of the cell to some location near the nucleus. The tip could then be used to move the nucleus within the punctured cell or to puncture the nucleus (Fig. 1). Occasionally, iontophoretic marking of the tip position (*13, 14*) was employed. After a successful entry, records such as trace 3 of Fig. 2 were again obtained when the whole epithelium was stimulated with subrheobase current pulses.

When the density of the overall stimulating current was increased above rheobase, the fast potential spikes were seen both in the transepithelial record (Fig. 3B, *V*-traces) and in the display of the potential between the microelectrode tip and outer solution (Fig. 3B, *v*-traces). When the outside solution was diluted Ringer, the spikes of both recordings often had almost identical amplitudes and time courses. Spikes were also recorded from cells lining the ducts of subepithelial glands. Only in occasional skins were the spike and the main resistive barrier found between first and second outer layers of cells. We suppose that the regenerative phase of these epithelia was closer to shedding of the outermost cell layer [(*10*), compare (*15*)].

In records of transepithelial potential the spike is usually followed by a second, although flat and drawn-out, peak (*1*). This peak is absent from many of our microelectrode recordings,

and may then indicate polarization at deeper levels of the epithelium.

In many of these recordings the spike appeared to be somewhat attenuated when compared with the response recorded across the whole epithelium. (In these cases the "missing" portion of the spike was seen in the simultaneous record of the potential between microelectrode tip and inside reference electrode. This is merely an algebraic necessity.) The attenuation is probably due to an incomplete seal between the microelectrode shaft and the punctured membrane. When the seal was improved by advancing the microelectrode (without the tip leaving the outermost cell layer), the attenuation became less and the spike residue disappeared from the potential difference between the tip and the inner reference electrode.

The appearance of the main portion of the spike between probing microelectrode and outer reference electrode may not unequivocally prove that the spike originates at the outermost membrane; it might also originate somewhere along a current pathway parallel to the one below the probing microelectrode tip. For instance, in Fig. 4B an increase of resistance $r_5$ without a corresponding increase of $r_2$ might force more current through $r_1$, such that at constant total current the potential difference ($v$) across $r_1$ reflects the changes of $r_5$. If $r_4$ were large, a spike caused by a change in $r_5$, would appear in $v$ with nearly the same attenuation (with respect to $V$) as a subrheobase potential response. If $r_4$ were smaller, the attenuation of the spike could even be larger than that of a subrheobase response, and if $r_4$ were 0, a change of $r_5$ would not be reflected in the potential across $r_1$ at all. On the other hand, if the spike amplitude of $v$ were found less attenuated with respect to that of $V$ than the subrheobase response, $r_5$ would be excluded as the sole origin of the spike,

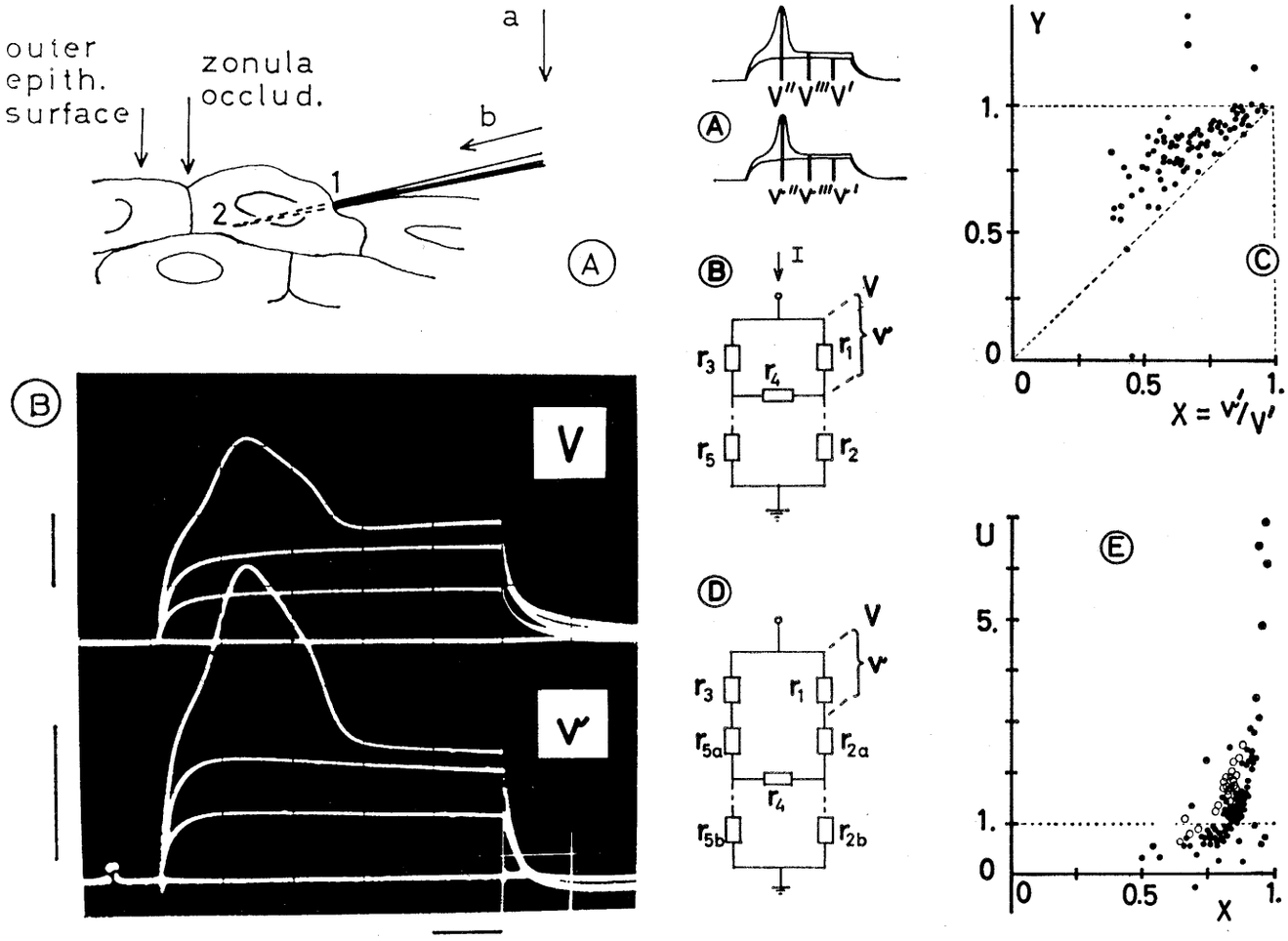


Fig. 3 (left). (A) Tip positions before (1) and after (2) entry; *a* and *b*, direction of first and second movement of probing microelectrode. (B) Simultaneous recordings of transepithelial potential ($V$) and potential ($v$) between outer solution and probing microelectrode tip while tip is in a surface cell. Density of three consecutive inward current pulses: 100, 200, and 300 $\mu$a/cm$^2$. Only the strongest current pulse was above rheobase. Vertical calibration 200 mv per interval. Probing electrode resistance calibration (pulse $A$): $4 \cdot 10^7$ ohms. Horizontal calibration: 5 msec per interval. Fig. 4 (right). (A) Transepithelial potential ($V$, above) and potential between outer solution and probing microelectrode tip ($v$, below), each recorded for a subrheobase ($I'$) and above rheobase ($I''$) current pulse. (B) Pathways of current entering through outer membranes ($r_1$ and $r_3$) of two neighboring surface cells, one of which has been punctured by the probing microelectrode to record $v$. (C) $Y = (v'' - v')/(V'' - V')$ is used for the amplitude ratio of spikes in the two recording channels. (D) Like (B), but major conductive cross-connection of neighboring cells is only present below outer cell layer. (E) $U = (V'/I' - V'''/I'') \cdot I'/(V' - v')$ is used to indicate relative magnitude of transepithelial resistance drop due to refractory state and resistance seen between tip and inside solution in the resting state. $U > 1$ means that the apparent resistance decrease connected with the refractory state was larger than the apparent resistance seen below the position of the microelectrode tip in the resting state. In this experiment, the outer solution was Ringer diluted tenfold.

although, theoretically, it might still contribute to the spike.

To test whether the spike was due to resistance changes in the lower branch of a parallel current pathway, the relative amplitudes of spikes and subrheobase responses of the $v$ and $V$ recording channels are displayed in Fig. 4C for 98 successive penetrations of the outer membrane. In this experiment, isotonic Ringer was used for the outside solution to lower the resting resistance of the outer membrane and thus obtain conditions more favorable to disprove the main conclusion of this paper.

In terms of Fig. 4B, the subrheobase potential ratio $X = (v'/V')$ is displayed on the abscissa and the ratio of spike amplitudes $Y = (v'' - v')/(V'' - V')$ on the ordinate of Fig. 4C. In most cases, $Y$ is found smaller than 1, and decreases with decreasing $X$. This is to be expected when a membrane leak around the microelectrode shaft lowers the original values of both $X$ and $Y$. Furthermore, $Y$ is generally larger than $X$, which excludes $r_5$ as the sole origin of the spike. Therefore, the spike, or at least its major part, must originate in $r_3$, $r_1$, or both, that is, outside the first major conductive cross-connection ($r_4$) between neighboring cells. The location of this connection cannot be seen from our experiments. However, it is likely to be the tight junction described for the outermost cell layer and termed zonula occludens (*15*). If there were no substantial cross-connection in the outermost cell layer, then the membranes between the first and second cell layers ($r_{5a}$ of Fig. 4D) could also be considered the sole origin of the spike.

The resistance decrease associated with the falling phase of the spike usually exceeds the increase associated with the rising phase, so that during the refractory period the total d-c resistance of the epithelium appears diminished below resting levels. If the spike were to originate at $r_{5a}$, the total resistance drop seen in the refractory period could not be larger than $r_{5a}$ itself. However, in 79 of 124 successive trials this total resistance decrease was even larger than the apparent resistance seen between tip and inner reference electrode in the resting state (Fig. 4E), a quantity which can be expected to exceed $r_{5a}$. The circles in Fig. 4E refer to recordings, where all of the sodium of the outer solution had been replaced by potassium. Then the response to a current pulse is merely delayed rectification, the resistance decrease of which can also be larger than the apparent resistance seen between microelectrode tip and inner reference electrode.

We conclude that in the epithelia studied the spike was generated at the outermost boundary of the surface cells. This corroborates the corresponding hypothesis of Finkelstein (*1*). We do not claim that the impaled cells were still excitable. A resistance increase restricted to most of the other surface cells would force sufficiently more current through the impaled cell to produce the recordings obtained. We have based our arguments on data from epithelia that showed little indication of non-*IR*-type potential changes (current, $I$; resistance, $R$). We assume that then the recorded potential changes reflect resistive phenomena. Further support for this must come from high time-resolution measurements of ohmic conductance changes in the presence of large parallel capacitances.

Our arguments are also based on the assumption that the spike is generated in but one of the series membranes of the epithelium. If several series membranes would spike, their thresholds and time constants would have to be quite similar, even soon after a change of the composition of the external solution, to produce the single-peaked spike records that we obtained. Such similarity we feel to be unlikely, particularly since we find the main resting resistance at the outermost membrane. In less than 0.3 percent of all skins that we investigated did we find a clearly double-peaked spike, which suggests that two series membranes were responding.

A main difference between the most superficial plasma membrane and deeper ones may be that, for lack of further cell layers on the outside facing membrane, the outermost plasma membrane proper is not shunted by maculae occludentes (*16*). Thus, while the spikes are normally seen only at the outermost membrane, the plasma membranes of cells below the surface layer might also show excitation once the shunting effect by the intercellular maculae occludentes is removed. However, even with the shunting maculae removed, a noticeable excitation would probably occur only if the sodium conductance (or more precisely the partial current of sodium) is predominating in the resting state. In frog skin, a large partial conductance for sodium may evolve gradually during the life cycle of any one epithelial cell.

B. LINDEMANN
U. THORNS

*2.Department of Physiology,*
*Saarland University,*
*665 Homburg/Saar, Germany*

### References and Notes

1. A. Finkelstein, *J. Gen. Physiol.* **47**, 545 (1964).
2. Suppose the excitable membrane behaved like a passive network with a resistance depending, for instance, on membrane potential. Then the spike would result from an interplay of potential and resistance at constant current, and the term resistance-potential-spike could be used and preferred over a term that mentions only one of the two important variables involved. The spike is probably of this nature. However, it must be admitted that changes of non-*IR*-type potentials (like phase boundary potentials and diffusion potentials at zero net current) may to a certain extent contribute to the recorded potential-time course. Such non-*IR*-type potential changes in frog skin are already evidenced by the tail portions of the records published by Finkelstein (*1*). Before their contribution is more carefully evaluated, we prefer the phenomenological term "potential spike." It may be added that, according to the definition given by Bullock and Horridge [T. H. Bullock and G. A. Horridge, *Structure and Function in the Nervous System of Invertebrates* (Freeman, San Francisco, California, 1965), vol. 2, pp. 1595 and 1608], Finkelstein was justified in applying the term "action potential" to the excitation phenomena described by him.
3. Abdominal skin of *Rana esculenta* was used in most cases. The experiments were done from March to July with unfed male animals, maintained at +4°C.
4. The staining is mentioned extensively because in experiments of others the dyes did not penetrate the skin [H. H. Ussing, *Ann. N.Y. Acad. Sci.* **137**, 543 (1966)].
5. A. C. MacRobbie and H. H. Ussing, *Acta Physiol. Scand.* **53**, 348 (1961).
6. J. Y. Lettwin, B. Howland, R. C. Gesteland, *IRE (Inst. Radio Eng.) Trans. Med. Electron.* **10**, 26 (1958).
7. To allow angles of more than 10 degrees, the water immersion objective was exchanged for a 32× objective with a working distance of 8 mm.
8. We thank Dr. R. O. Eckert for helpful discussions and for the use of certain equipment.
9. Accurate tip movements in 1-$\mu$ steps were effected with a step motor coupled, with reduction, to the axial drive of the electrode holder and driven by a Tektronix pulse generator.
10. A closer correlation to the stage of regeneration must be attempted in the future.
11. T. Hoshiko, in *Biophysics of Physiological and Pharmacological Actions*, A. M. Shanes, Ed. (AAAS, Washington, D.C., 1961), p. 46.
12. Basically similar results are obtained when the outer solution is diluted Ringer. With tips 1 and 2 pushed into the same surface cell, we find the signal increased by several hundred percent, which indicates a higher "input resistance" than before. While there can be a number of reasons for this phenomenon, it certainly shows that tip 1 delivers current when inside the cell.
13. G. Whittembury, *J. Gen. Physiol.* **47**, 795 (1964).
14. R. C. Thomas and V. J. Wilson, *Science* **151**, 1538 (1966).
15. M. G. Farquhar and G. E. Palade, *Proc. Nat. Acad. Sci. U.S.* **51**, 569 (1964).
16. In the resting state, the shunting effect of zonulae occludentes is probably small [(*15*) and H. H. Ussing and E. E. Windhager, *Acta Physiol. Scand.* **64**, 484 (1964)]. Additional shunting of the surface layer by flask cells and duct lumina of multicellular glands is difficult to evaluate.
17. Supplied by the Deutsche Forschungsgemeinschaft. A more detailed report will appear elsewhere.

9 August 1967